

Thermally Stable Carbazole Tagged Au(I)- Mesoionic N-Heterocyclic Carbene Complexes with Diverse Gold-Hydrogen Bonds

Subramaniyam Kalaivanan,^a Vaddamanu Moulali,^a Kumar Siddhant,^b Kavitha Velappan,^c Kyohei Hisano,^b Osamu Tsutsumi^{*b} and Ganesan Prabusankar^{*,a}

^aDepartment of Chemistry, Indian Institute of Technology Hyderabad, Hyderabad, Kandi, Telangana, INDIA 502285. E-mail: prabu@chy.iith.ac.in

^bDepartment of Applied Chemistry, Ritsumeikan University, Kusatsu 525-8577, JAPAN. E-mail: tsutsumi@sk.ritsumei.ac.jp

^cDAV-IITH, Indian Institute of Technology Hyderabad, Kandi, Telangana, INDIA-502 284.

Supporting Information

Contents	Table of contents	Page. No
Figure S1	FT-IR (neat, $\bar{\nu}$) spectrum of L¹.HI .	2
Figure S2	¹ H NMR spectrum of L¹.HI in DMSO- <i>d</i> ₆ at 27 °C.	3
Figure S3	¹³ C NMR spectrum of L¹.HI in DMSO- <i>d</i> ₆ at 27 °C.	4
Figure S4	FT-IR (neat, $\bar{\nu}$) spectrum of L².HI .	5
Figure S5	¹ H NMR spectrum of L².HI in DMSO- <i>d</i> ₆ at 27 °C.	6
Figure S6	¹³ C NMR spectrum of L².HI in DMSO- <i>d</i> ₆ at 27 °C.	7
Figure S7	FT-IR (neat, $\bar{\nu}$) spectrum of 1 .	8
Figure S8	¹ H NMR spectrum of 1 in CDCl ₃ at 27 °C.	9
Figure S9	¹³ C NMR spectrum of 1 in CDCl ₃ at 27 °C.	10
Figure S10	FT-IR (neat, $\bar{\nu}$) spectrum of 2 .	11
Figure S11	¹ H NMR spectrum of 2 in CDCl ₃ at 27 °C.	12
Figure S12	¹³ C NMR spectrum of 2 in CDCl ₃ at 27 °C.	13
Figure S13	The solid-state structure of L¹.HI .	13
Figure S14	Contour line diagrams of the Laplacian distribution $\nabla^2\rho(r)$ of 1A .	14
Table S1	Cartesian Coordinates of 1A .	15
Table S2	Excitation energies and oscillator strengths of 1A .	17
Table S3	Nature of bonding Au-Carbene bond (from NBO analysis) of 1A .	20
Table S4	Crystallographic data for L¹.HI .	20
Table S5	The selected bond lengths (Å) and angles (°) and of L¹.HI .	21

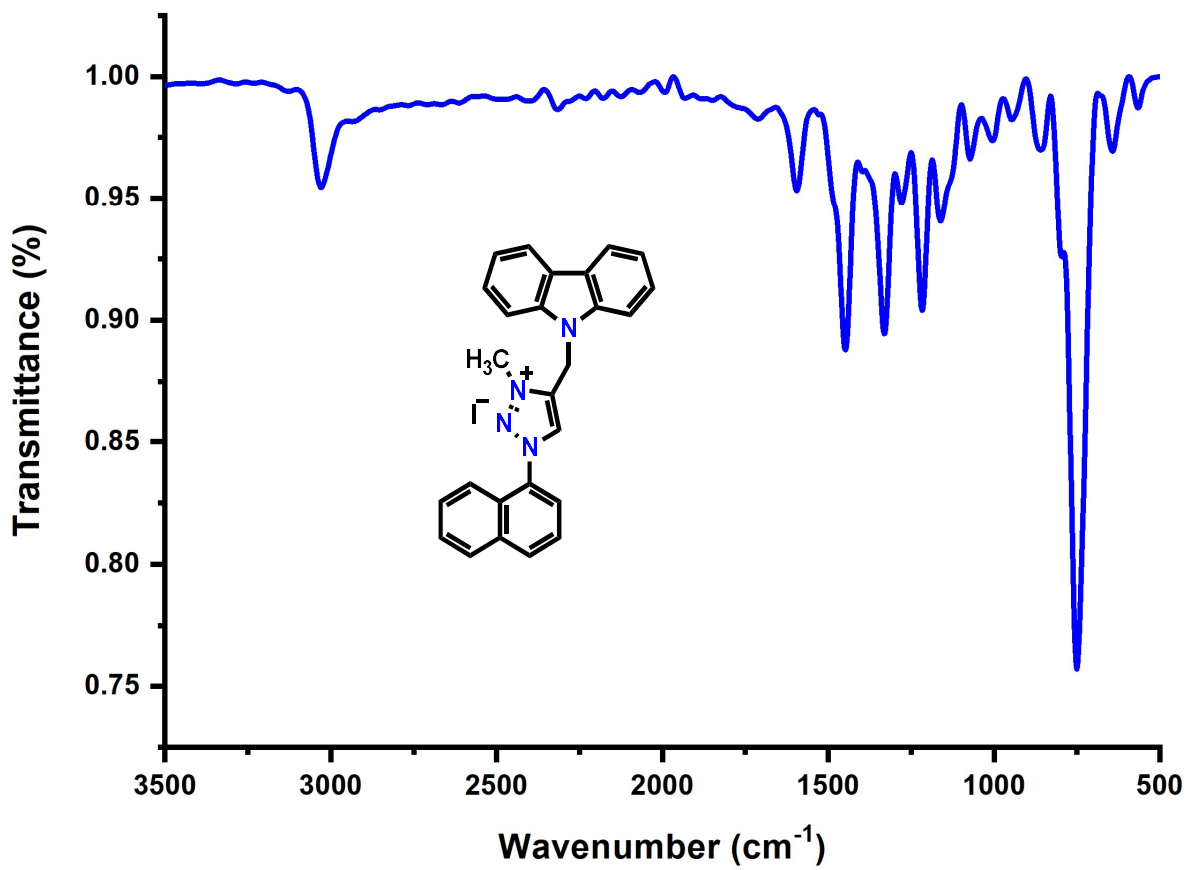


Fig. S1. FT-IR (neat, $\bar{\nu}$) spectrum of L¹.HI.

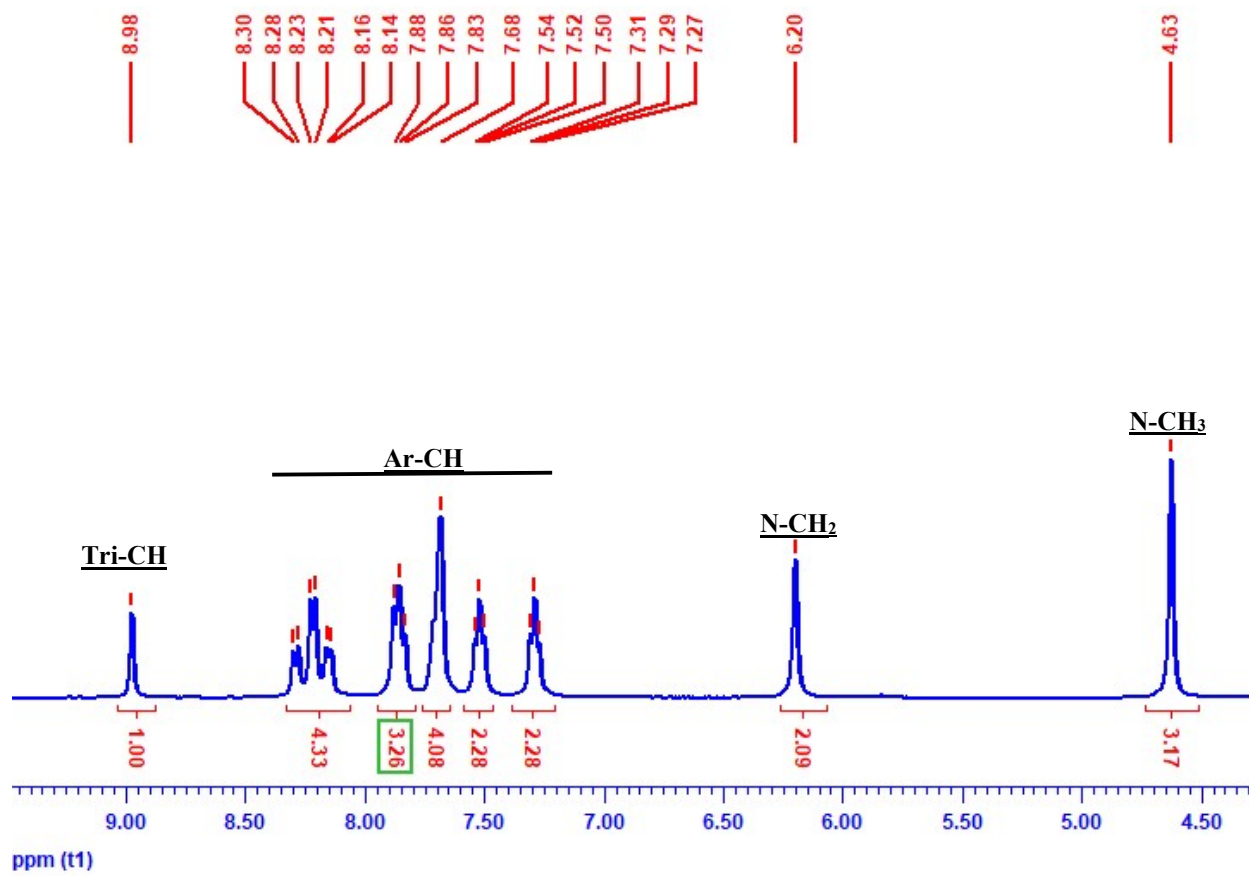


Fig. S2. ^1H NMR spectrum of $\text{L}^1\cdot\text{HI}$ in $\text{DMSO-}d_6$ at $27\text{ }^\circ\text{C}$.

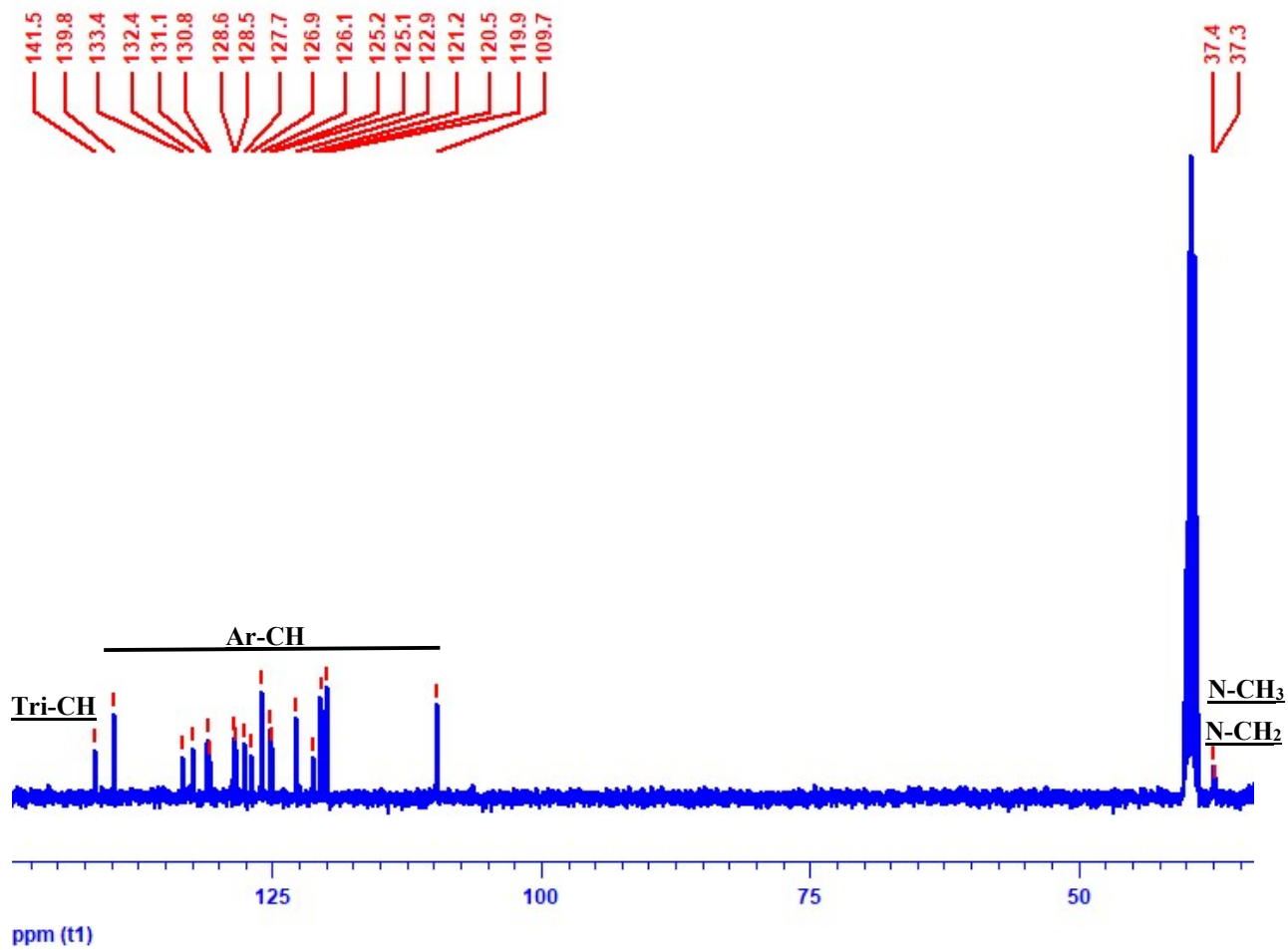


Fig. S3. ^{13}C NMR spectrum of $\text{L}^1\cdot\text{HI}$ in $\text{DMSO-}d_6$ at 27°C .

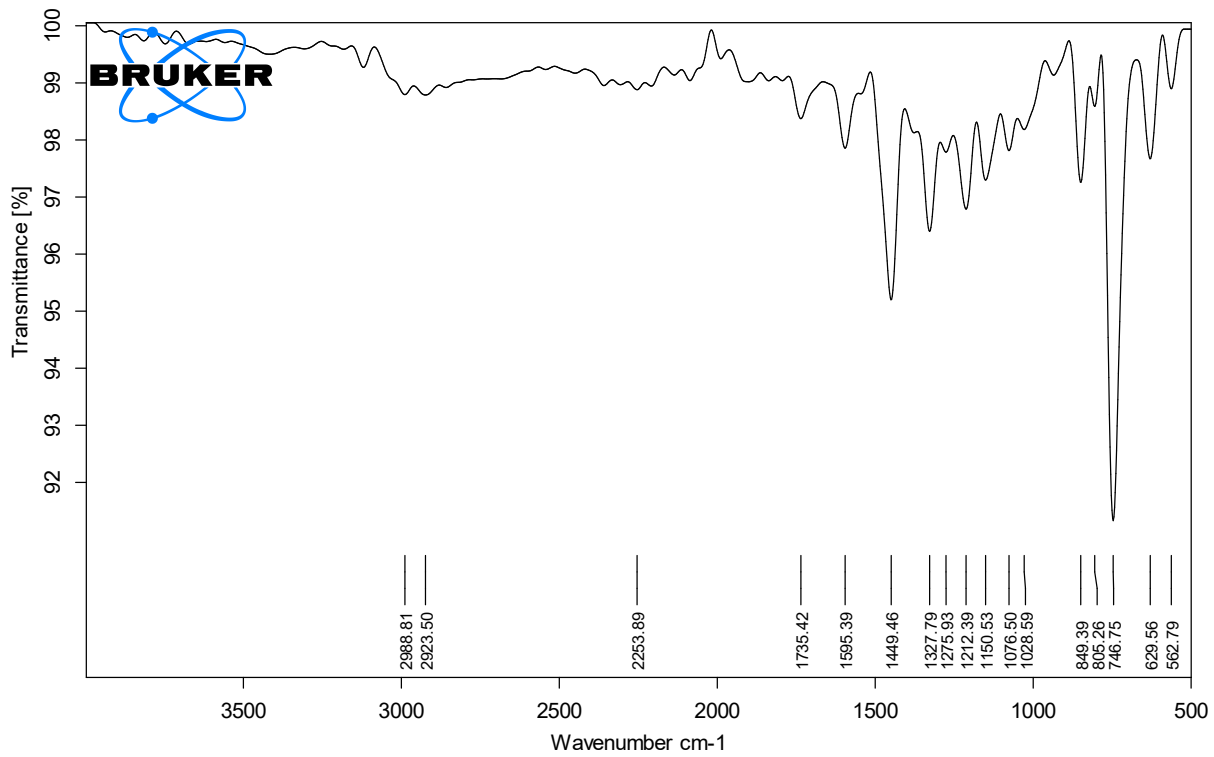


Fig. S4. FT-IR (neat, $\bar{\nu}$) spectrum of L².HI.

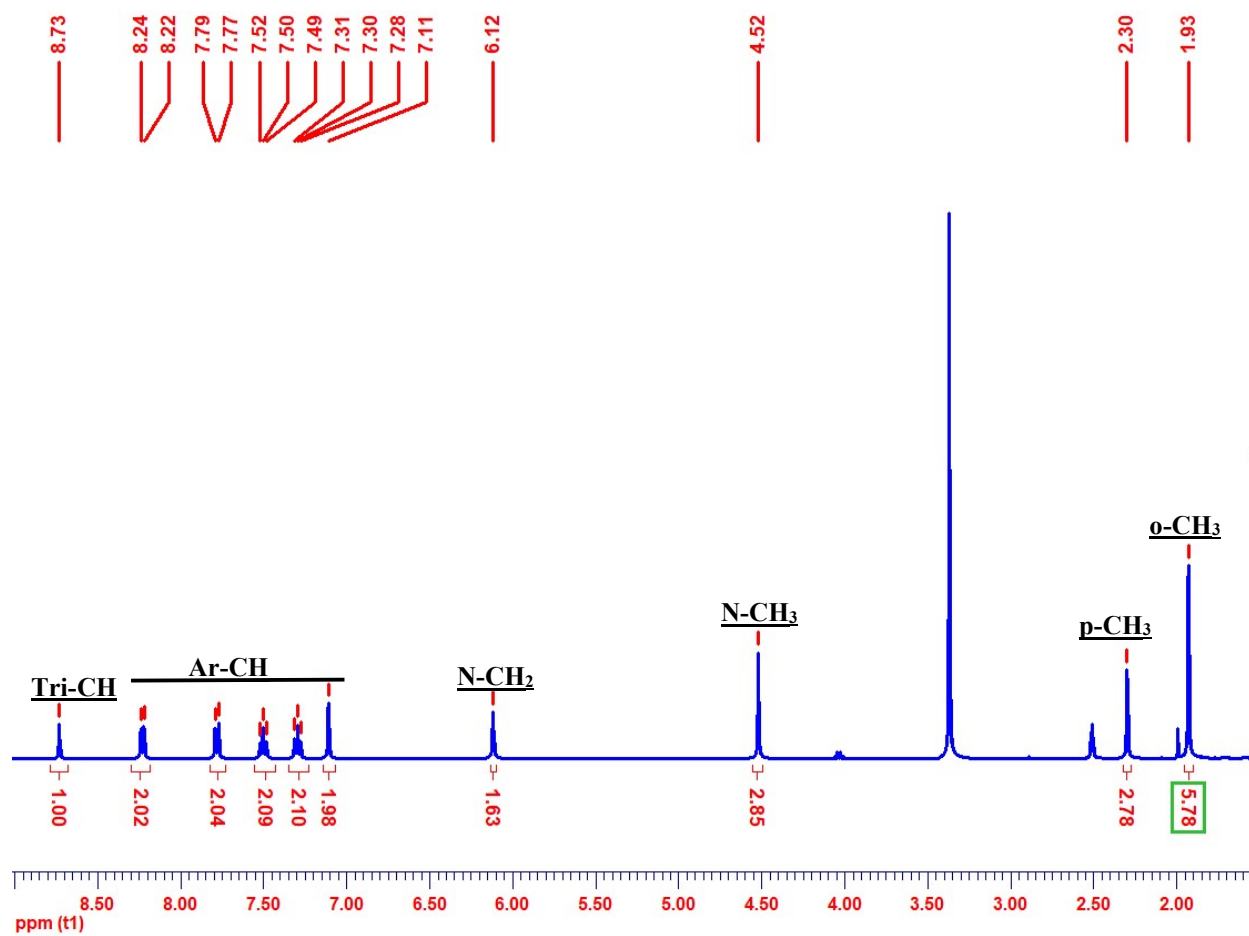


Fig. S5. ^1H NMR spectrum of $\text{L}^2\cdot\text{HI}$ in $\text{DMSO-}d_6$ at 27°C .

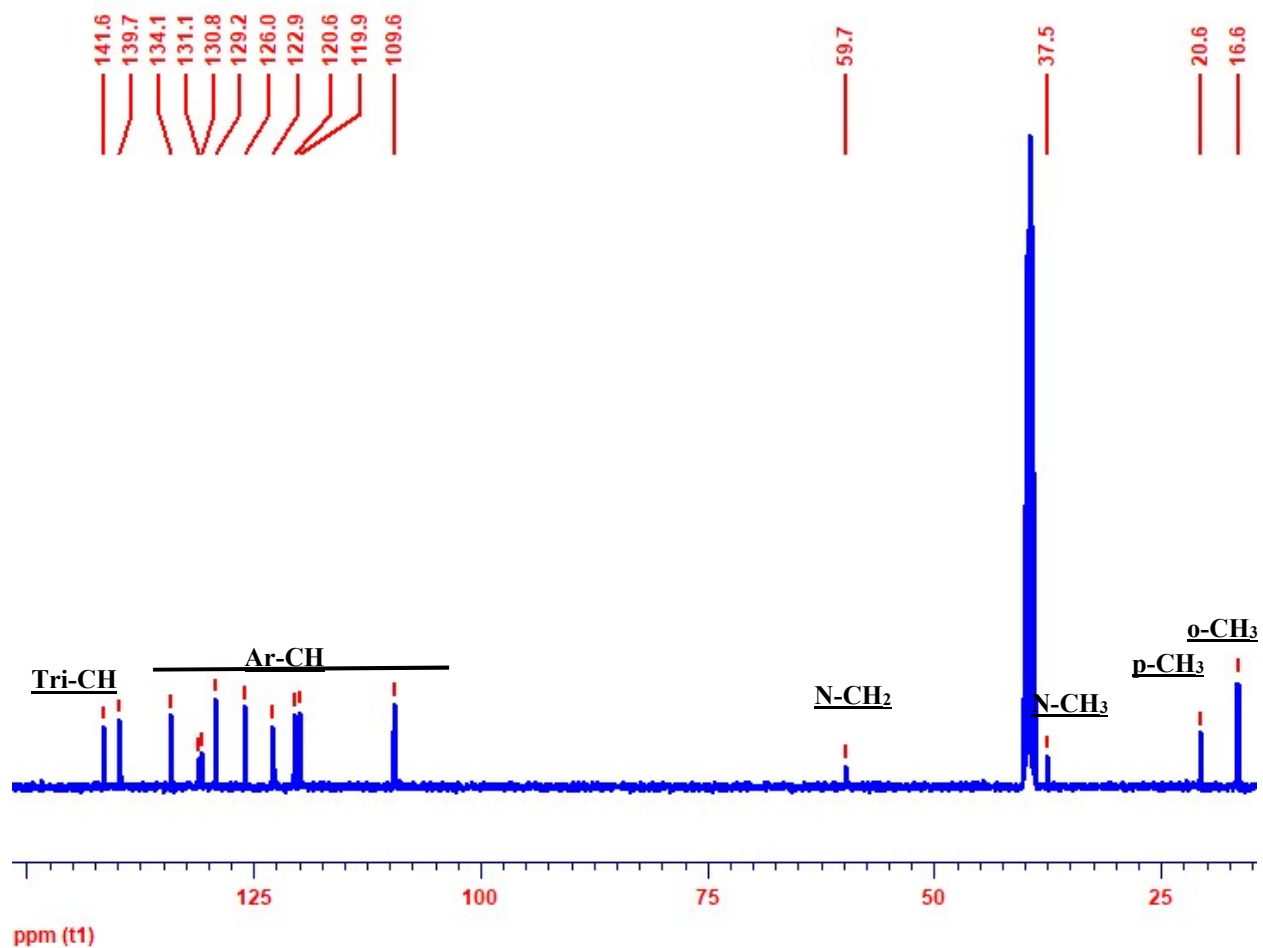


Fig. S6. ¹³C NMR spectrum of L².HI in DMSO-*d*₆ at 27 °C.

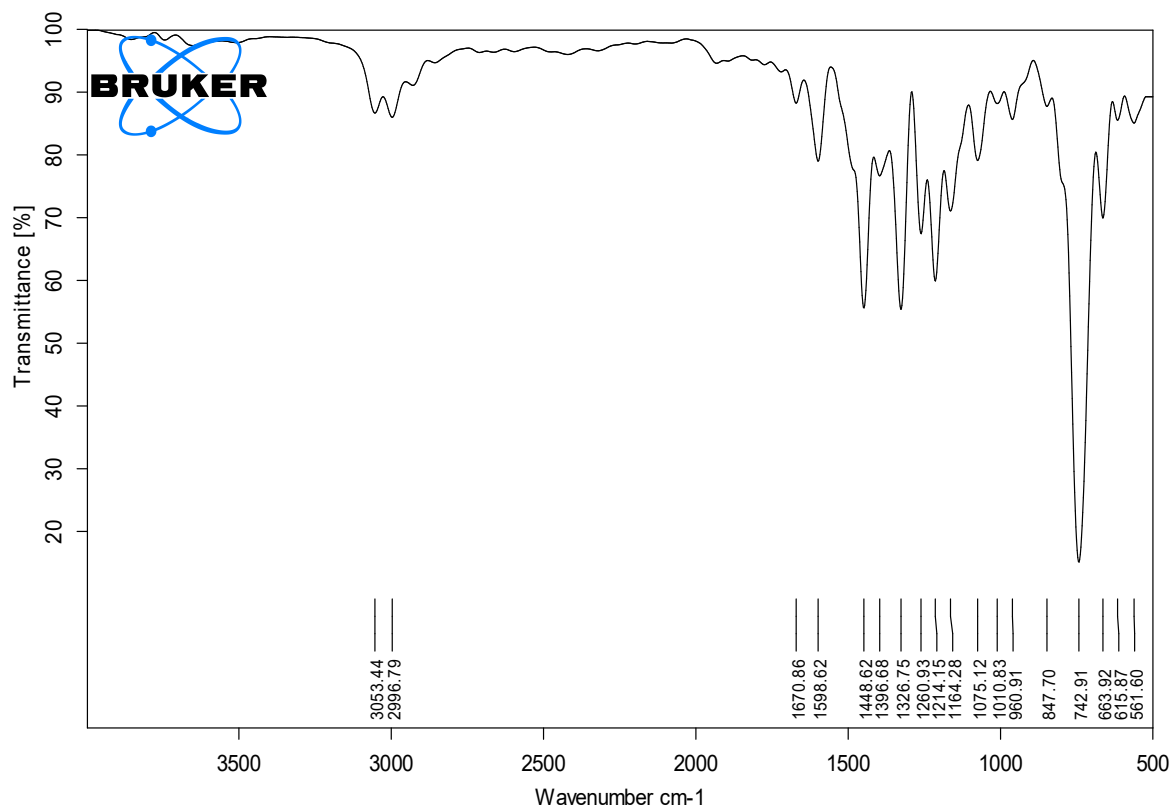


Fig. S7. FT-IR (neat, $\bar{\nu}$) spectrum of **1**.

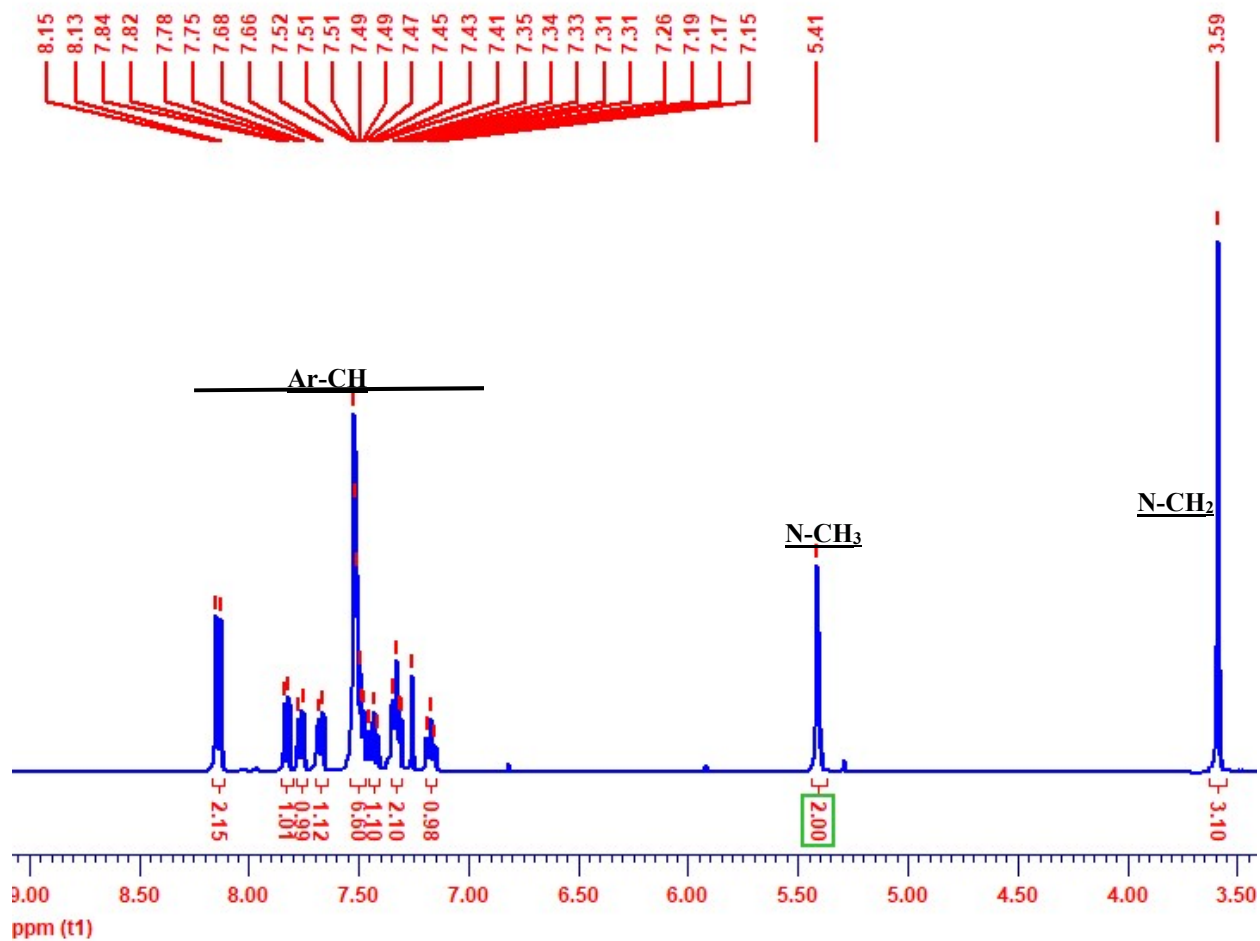


Fig. S8. ^1H NMR spectrum of **1** in CDCl_3 at $27\text{ }^\circ\text{C}$.

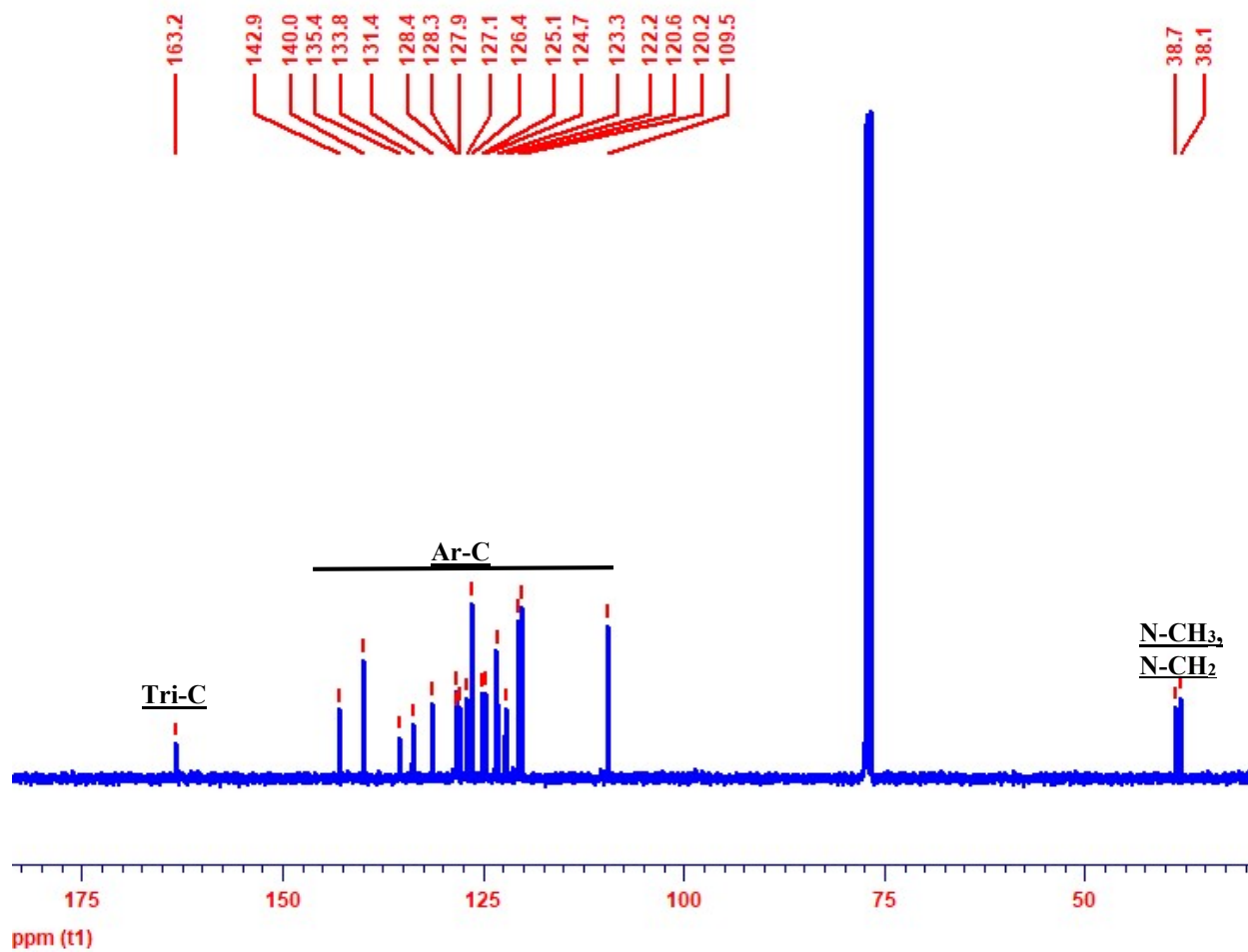


Fig. S9. ^{13}C NMR spectrum of **1** in CDCl_3 at 27 °C.

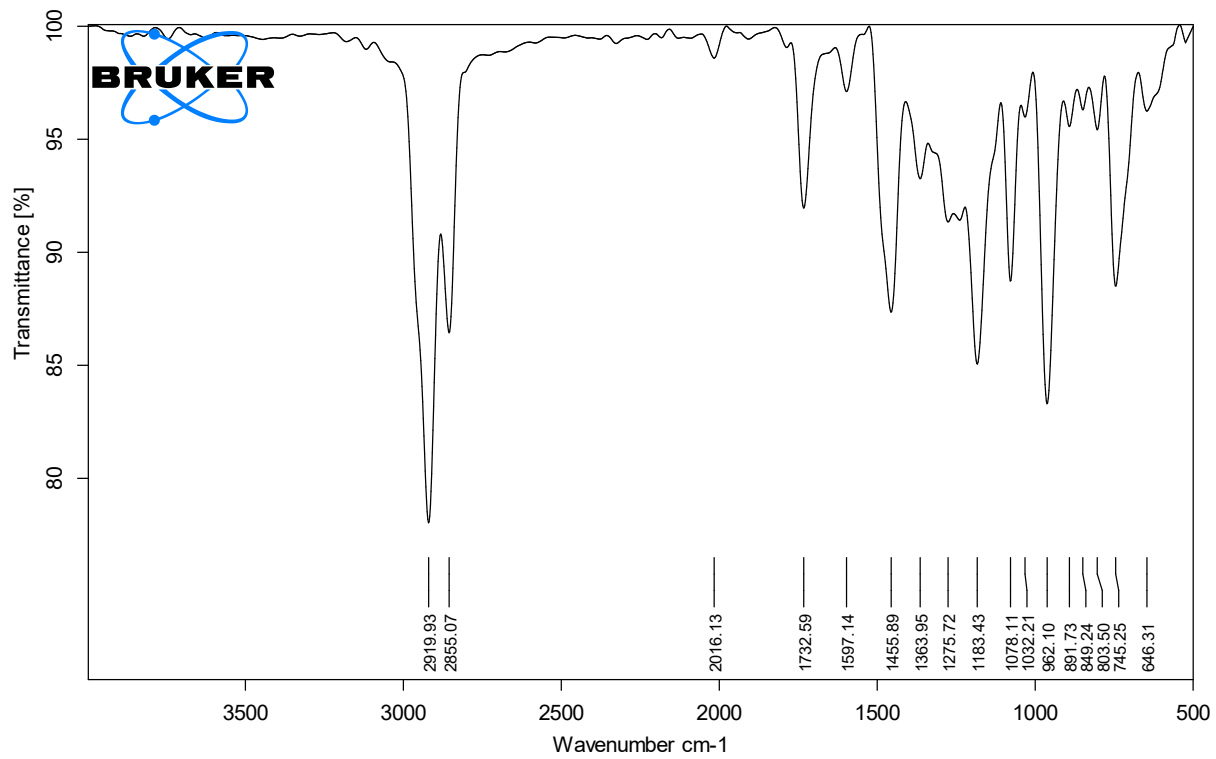


Fig. S10. FT-IR (neat, $\bar{\nu}$) spectrum of **2**.

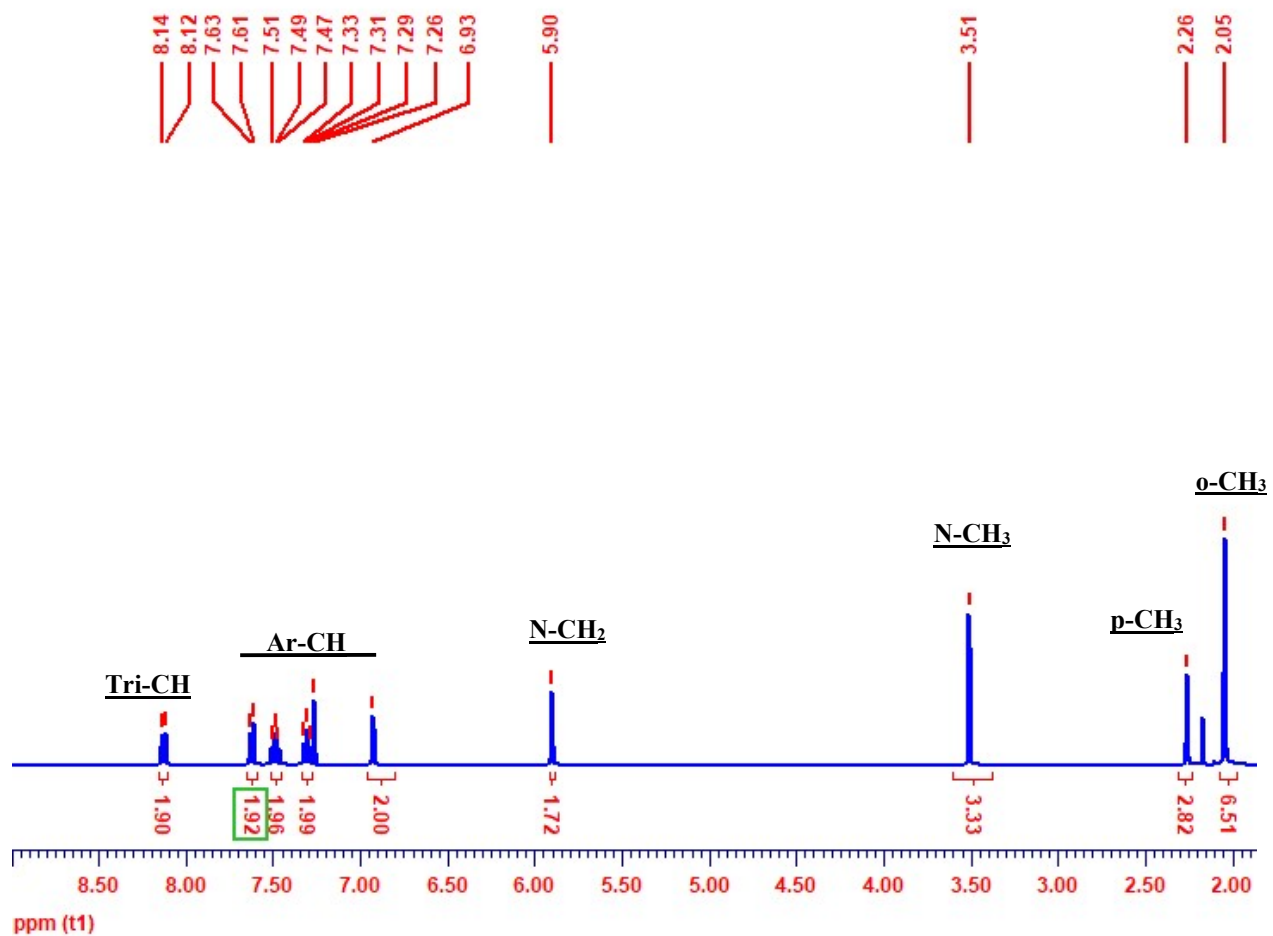


Fig. S11. ^1H NMR spectrum of **2** in CDCl_3 at 27°C .

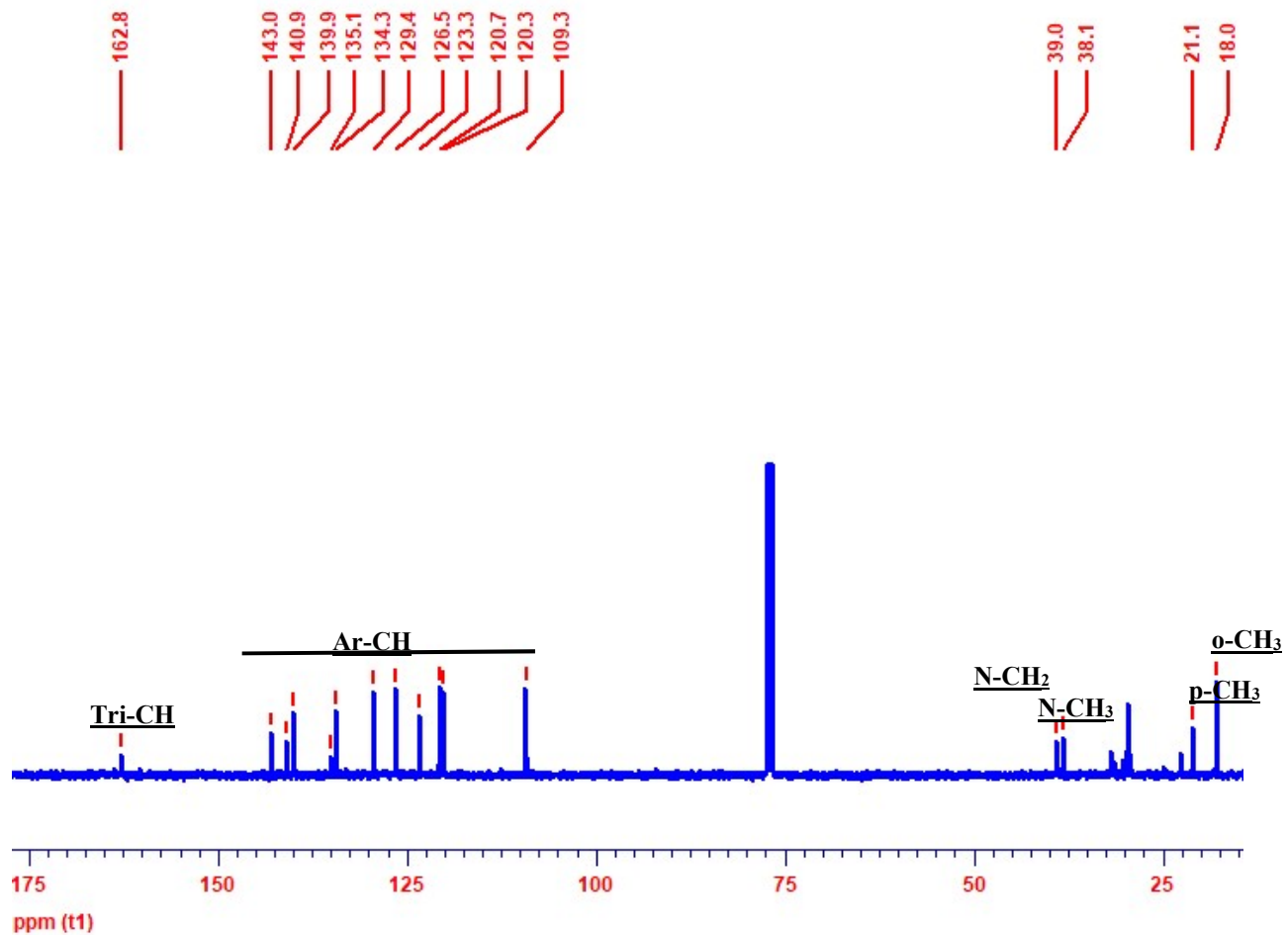


Fig. S12. ^{13}C NMR spectrum of **2** in CDCl_3 at 27 $^\circ\text{C}$.

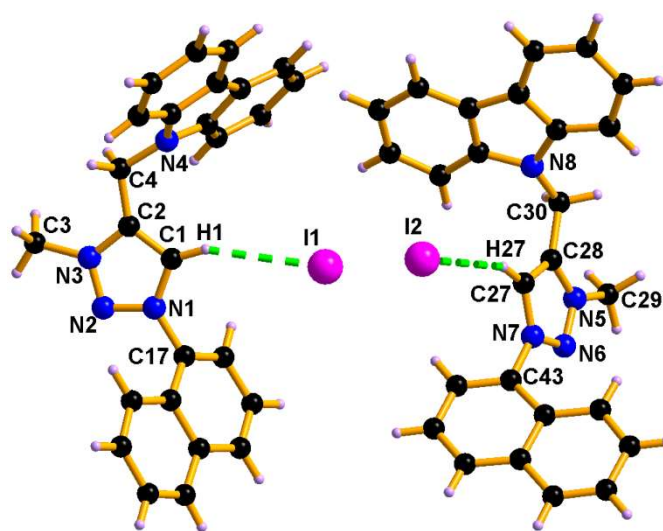


Figure S13. The solid-state structure of $\text{L}^1\cdot\text{HI}$.

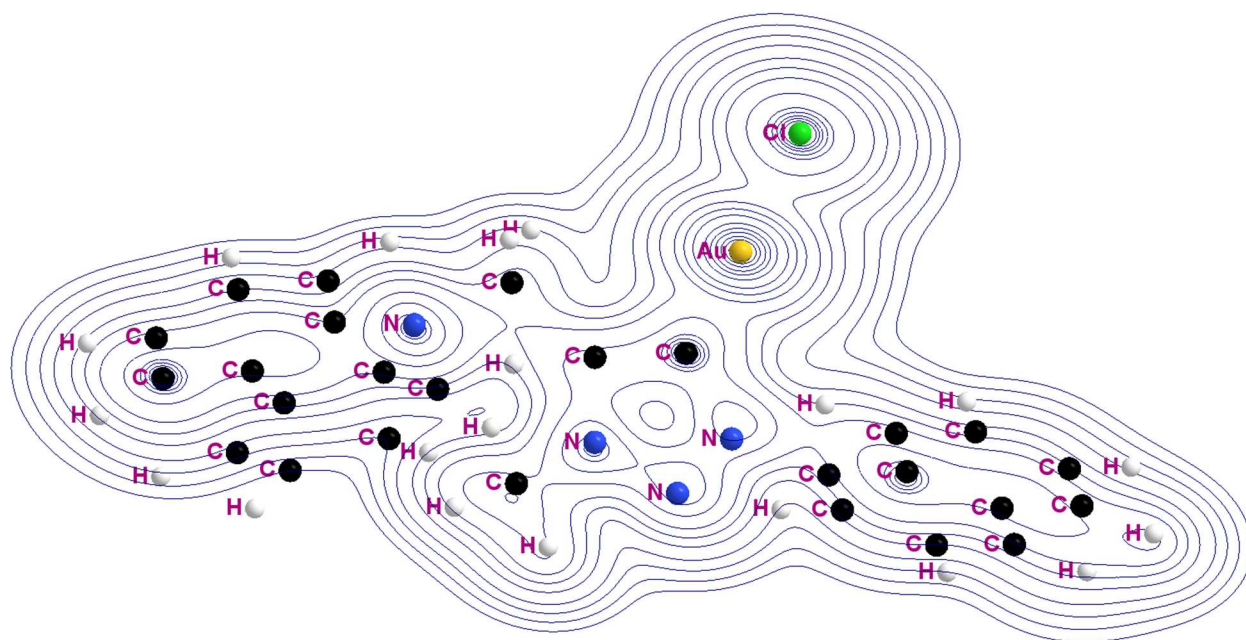


Fig. S14. Contour line diagrams of the Laplacian distribution $\nabla^2\rho(r)$ of **1A**.

Table S1. Cartesian Coordinates of **1A**.

ATOM	X	Y	Z
Au	3.5055581876	5.1288217905	15.880062006
Cl	3.6106410045	5.0287909829	18.1870442556
N	6.873217111	5.5405005841	12.4707314104
N	2.4078611635	4.8729870506	13.0439382004
N	3.8915446322	5.4861785066	11.7087669133
N	2.6587717968	5.0209263049	11.7422787673
C	7.6936166473	6.1866188919	11.5444767074
C	5.813317766	6.1499372149	13.2532605707
H	5.8531386767	7.2310880591	13.0910957844
H	5.9834784862	5.9899751159	14.3239421798
C	3.4563831896	5.2179701819	13.8721746184
C	7.2657430208	4.2026807568	12.5604479177
C	-0.032811428	5.200586279	13.3088513497
C	8.6078243423	5.2412335074	11.0039616915
C	4.4319903711	5.6238528316	12.9581347207
C	0.009346161	6.5391218666	12.8315494177
H	0.9578566094	6.9720625839	12.5341958476
C	1.1144514122	4.3644697709	13.4336675523
C	7.7033873192	7.5259449912	11.1365543577
H	7.0244283996	8.2617475785	11.5571639973
C	8.3337756521	3.9744860177	11.6539801763
C	-1.2937555079	4.6471977092	13.7143062256
C	-1.3460001854	3.3207584019	14.2229050211
H	-2.3072587409	2.9188309047	14.5313608339
C	4.4986906834	5.7322557688	10.3985435204
H	5.2872881814	5.0006338896	10.2153562489
H	4.924007365	6.7364201019	10.3719187225
H	3.7104574959	5.6357385208	9.6533356979
C	1.0432886128	3.0851385396	13.9357810039
H	1.9476279597	2.49396584	14.0308294028
C	6.7628948355	3.1880406681	13.3828709567
H	5.9615026286	3.3691418569	14.0919145344
C	9.5362498265	5.6517254159	10.0387279548
H	10.2431148257	4.9411678559	9.6196027084
C	8.8988641756	2.6953329287	11.5638576119
H	9.719251717	2.5012356452	10.878624227
C	-0.2054305254	2.5572034375	14.3372138718
H	-0.2533432867	1.5498877183	14.7377449757
C	-2.4619602374	5.4515916268	13.6074967014
H	-3.4146605518	5.0277960579	13.9135145481
C	8.6400101808	7.9087903075	10.1738768285
H	8.6695552918	8.9445764042	9.8485562893

C	7.3467399203	1.9248429325	13.2747000248
H	6.9823854234	1.120052363	13.9062480572
C	8.3992725237	1.6765032862	12.3738558007
H	8.8306718102	0.6817737059	12.3170643271
C	9.5468421089	6.9837464263	9.6260493941
H	10.2642424059	7.3136103487	8.8810045653
C	-1.1429012135	7.2910673485	12.7493006421
H	-1.0939462248	8.3142997898	12.3886911178
C	-2.391673423	6.7434101552	13.1349354091
H	-3.2905485965	7.3482831776	13.0625343347

Table S2. Excitation energies and oscillator strengths of **1A**.

Orbitals involved in the transition		Energy, eV	Wavelength, nm	Oscillator strength
HOMO-1→LUMO	0.23578 (11%)	3.3781	367.03 nm	0.0011
HOMO→LUMO	0.63523 (80%)			
HOMO→LUMO+1	-0.16777 (5%)			
HOMO-2→LUMO	-0.11807 (2%)	3.4773	356.56 nm	0.0227
HOMO-1→LUMO	0.63943 (82%)			
HOMO→LUMO	-0.26146 (13%)			
HOMO-5→LUMO	0.66387 (88%)	3.9724	312.12 nm	0.0105
HOMO-5→LUMO+1	-0.13657 (4%)			
HOMO-4→LUMO+1	0.10155 (2%)			
HOMO-3→LUMO+5	0.15806 (5%)	3.9860	311.05 nm	0.0404
HOMO-2→LUMO+2	-0.15748 (5%)			
HOMO-1→LUMO+2	0.27826 (15%)			
HOMO→LUMO+2	0.59044 (70%)			
HOMO-5→LUMO+1	0.27918 (15%)	4.1663	297.59 nm	0.0337
HOMO-4→LUMO	0.19758 (8%)			
HOMO-4→LUMO+1	0.60575 (73%)			
HOMO-6→LUMO	0.16506 (5%)	4.3583	284.48 nm	0.0462
HOMO-6→LUMO+1	0.14636 (4%)			
HOMO-5→LUMO	0.11686 (2%)			
HOMO-5→LUMO+1	0.53224 (56%)			
HOMO-4→LUMO+1	-0.22736 (10%)			
HOMO-4→LUMO+3	0.23526 (11%)			
HOMO-6→LUMO	0.36485 (27%)	4.3987	281.86 nm	0.0103
HOMO-6→LUMO+1	0.26317 (14%)			
HOMO-5→LUMO+1	-0.31630 (20%)			
HOMO-5→LUMO+3	-0.13741 (4%)			
HOMO-4→LUMO+3	0.34018 (23%)			
HOMO-2→LUMO+3	0.11074 (2%)			
HOMO-1→LUMO+3	-0.10386 (2%)			
HOMO-3→LUMO+2	0.60943 (74%)	4.4254	280.17 nm	0.1050
HOMO-1→LUMO+5	-0.12546 (3%)			
HOMO→LUMO+4	-0.12766 (3%)			
HOMO→LUMO+5	-0.23419 (11%)			
HOMO-1→LUMO+3	0.50073 (50%)	4.5022	275.39 nm	0.0132
HOMO→LUMO+3	-0.48471 (47%)			
HOMO-6→LUMO	0.38642 (30%)	4.6358	267.45 nm	0.0180
HOMO-6→LUMO+1	-0.23992 (11%)			
HOMO-2→LUMO+3	-0.31362 (20%)			
HOMO-1→LUMO+3	0.27374 (15%)			

HOMO→LUMO+3	0.29188 (17%)			
HOMO-2→LUMO+4	-0.12440 (3%)	4.7779	259.49 nm	0.0220
HOMO-1→LUMO+4	0.24208 (12%)			
HOMO→LUMO+3	0.12178 (3%)			
HOMO→LUMO+4	0.58781 (69%)			
HOMO→LUMO+5	-0.11525 (2%)			
HOMO-10→LUMO	0.12595 (3%)	4.9443	250.76 nm	0.0126
HOMO-2→LUMO+6	-0.12130 (3%)			
HOMO-1→LUMO+4	0.58432 (69%)			
HOMO-1→LUMO+6	-0.16570 (5%)			
HOMO→LUMO+4	-0.24414 (12%)			
HOMO-2→LUMO+4	-0.23190 (11%)	5.0156	247.20 nm	0.0703
HOMO-2→LUMO+6	-0.22331 (10%)			
HOMO-1→LUMO+6	0.54438 (59%)			
HOMO→LUMO+5	0.15014 (4%)			
HOMO-6→LUMO+1	-0.12540 (3%)	5.0354	246.23 nm	0.0229
HOMO-5→LUMO+3	0.53384 (57%)			
HOMO-4→LUMO+3	0.36107 (26%)			
HOMO-4→LUMO+6	0.11527 (2%)			
HOMO→LUMO+6	0.10812 (2%)			
HOMO-7→LUMO+2	-0.10274 (2%)	5.0639	244.84 nm	0.1132
HOMO-3→LUMO+2	-0.11944 (2%)			
HOMO-3→LUMO+3	0.13276 (3%)			
HOMO-3→LUMO+4	0.48306 (46%)			
HOMO-3→LUMO+11	0.11017 (2%)			
HOMO-2→LUMO+6	-0.10265 (2%)			
HOMO-1→LUMO+5	-0.10048 (2%)			
HOMO→LUMO+5	-0.34137 (23%)			
HOMO-2→LUMO+4	0.53354 (57%)	5.0717	244.46 nm	0.0375
HOMO-2→LUMO+6	0.23293 (11%)			
HOMO-1→LUMO+4	0.11770 (2%)			
HOMO-1→LUMO+6	0.29529 (17%)			
HOMO-11→LUMO	0.10537 (2%)	5.0855	243.80 nm	0.1585
HOMO-7→LUMO+1	-0.13375 (3%)			
HOMO-3→LUMO+2	0.13975 (3%)			
HOMO-3→LUMO+4	0.43364 (37%)			
HOMO-1→LUMO+5	0.11409 (2%)			
HOMO-1→LUMO+6	-0.12897 (3%)			
HOMO→LUMO+5	0.34888 (24%)			
HOMO-11→LUMO	-0.29855 (18%)	5.0977	243.22 nm	0.0341
HOMO-11→LUMO+1	-0.14850 (4%)			

HOMO-9→LUMO+1	0.17662 (6%)			
HOMO-7→LUMO	0.11778 (2%)			
HOMO-7→LUMO+1	0.49310 (48%)			
HOMO-6→LUMO+1	0.16565 (5%)			
HOMO→LUMO+5	0.15341 (5%)			

Table S3. Nature of bonding Au-Carbene bond (from NBO analysis) of **1A**.

NBO	Occupancy	Coefficients		Hybrids
$\sigma_{\text{Au1-C11}}$	1.95744	23.35%	0.4832* Au1	s(78.86%)p 0.04(3.11%)d 0.23(17.95%)f0.00(0.09%)
		76.65%	0.8755* C11	s(37.83%)p 1.64(62.17%)d 0.00(0.00%)

Table S4. Crystallographic data for **L¹.HI**.

Identification code	L¹.HI
Empirical formula	C ₂₆ H ₂₁ IN ₄
Formula weight	516.388
Temperature/K	298.0
Crystal system	monoclinic
Space group	P2 ₁ /c
a/Å	7.2137(3)
b/Å	27.0679(10)
c/Å	22.9078(7)
α /°	90
β /°	90.190(3)
γ /°	90
Volume/Å ³	4473.0(3)
Z	8
ρ_{calcd} g/cm ³	1.534
μ /mm ⁻¹	1.452
F (000)	2061.9
Crystal size/mm ³	0.074 × 0.054 × 0.016
Radiation	Mo K α (λ = 0.71073)
2 Θ range for data collection/°	5.64 to 58.28
Index ranges	-9 ≤ h ≤ 8, -31 ≤ k ≤ 36, -31 ≤ l ≤ 24
Reflections collected	38669
Independent reflections	9968 [R _{int} = 0.0579, R _{sigma} = 0.0481]
Data/restraints/parameters	9968/0/561
Goodness-of-fit on F ²	1.022
Final R indexes [I ≥ 2 σ (I)]	R ₁ = 0.0345, wR ₂ = 0.0738
Final R indexes [all data]	R ₁ = 0.0540, wR ₂ = 0.0800
Largest diff. peak/hole / e Å ⁻³	0.87/-0.75

Table S5. The selected bond lengths (Å) and angles (°) and of **L¹.III**.

Bond Lengths (Å)	
N3-N2	1.314(3)
N3-C2	1.355(3)
N3-C3	1.451(3)
N1-N2	1.327(3)
N1-C1	1.354(3)
N1-C17	1.442(3)
C1-C2	1.362(4)
C2-C4	1.486(4)
Au1-Cl1	-
Au1-C1	-
Bond Angles (°)	
C1-N1-C17	128.8(2)
C1-C2-C4	134.0(2)
N2-N3-C2	113.1(2)
N2-N1-C1	112.4(2)
N1-C1-C2	105.6(2)
N3-C2-C1	105.0(2)
N3-N2-N1	103.82(19)
C1-Au1-Cl1	-
